

**PROCEEDINGS OF THE 2000 DOE/NREL HYDROGEN PROGRAM REVIEW**

**MAY 8-10, 2000**

**CARBON NANOTUBE MATERIALS FOR HYDROGEN STORAGE**

A.C. Dillon, T. Gennett, J. L. Alleman, K.M. Jones, P.A. Parilla,  
and M.J. Heben

National Renewable Energy Laboratory  
Golden, CO 80401-3393

**Abstract**

Carbon single-wall nanotubes (SWNTs) are capable of adsorbing hydrogen quickly, to high density, at ambient temperatures and pressures. Last year, we showed that hydrogen storage densities on SWNTs made by laser vaporization ranged from 3.5 to 4.5 wt% after a new cutting procedure was performed. We present the details of the cutting procedure here and show that, when optimized, hydrogen storage densities up to 7 wt% can be achieved. Infrared absorption spectroscopy measurements on pristine and H<sub>2</sub>-charged samples indicate that no C-H bonds are formed in the hydrogen adsorption process. These experiments are in agreement with an earlier temperature programmed desorption analysis which showed that hydrogen molecules are not dissociated when bound to the SWNT surfaces<sup>1</sup>. This conclusion is further supported by the first neutron scattering measurements which were performed through collaboration with researchers at NIST and University of Pennsylvania<sup>2</sup>. We also developed methods to tune SWNT diameters during synthesis so that mechanistic aspects of H<sub>2</sub> storage can be probed<sup>3</sup>, and learned how to de-tangle and organize individual tubes to form "superbundles" that will afford high volumetric storage densities<sup>4</sup>. Finally, we wish to report that we have performed first synthesis experiments with a new laser which recently arrived at NREL. Raman spectroscopy indicated that the as-produced materials were ~ 50 wt% pure SWNTs, in contrast to the 20 to 30 wt% usually seen with the previous laser, and the production rate for raw soot appears to be significantly greater than the 150 mg/hr observed previously, even though the current performance is probably far from optimal.

## **Statement of the Problem / Relevance of the Work**

### **Background**

With the 1990 Clean Air Act and the 1992 Energy Policy Act, the United States recognized the need for a long-term transition strategy to cleaner transportation fuels<sup>5</sup>. This realization comes while the U.S. continues to increase petroleum imports beyond 50% of total oil consumption, with nearly 50% of the total oil consumed being used in the transportation sector<sup>6</sup>. Because of the potential for tremendous adverse environmental, economic, and national security impacts, fossil fuels must be replaced with pollution-free fuels derived from renewable resources. Hydrogen is an ideal candidate as it is available from domestic renewable resources, and usable without pollution. It could therefore provide the long-term solution to the problems created by the Nation's dependence on fossil fuel.

Interest in hydrogen as a fuel has grown dramatically since 1990, and many advances in hydrogen production and utilization technologies have been made. However, hydrogen storage technology must be significantly advanced in performance and cost effectiveness if the U.S. is to establish a hydrogen based transportation system. As described in the U.S. DOE Hydrogen Program Plan for FY 1993 - FY 1997, compact and lightweight hydrogen storage systems for transportation do not presently exist.

Hydrogen provides more energy than either gasoline or natural gas on a weight basis. It is only when the weight, volume, and round-trip energy costs of the entire fuel storage system and charging/discharging cycle is considered that hydrogen's drawbacks become apparent. New approaches enabling more compact, lightweight, and energy efficient hydrogen storage are required in order for the wide-spread use of hydrogen powered vehicles to become a reality.

Research and development geared towards implementation of a national hydrogen energy economy has many indirect economic benefits. With almost 600 million vehicles in the world in 1992 - double the number in 1973 - the conflict between energy requirements, power generation, and environmental concerns is felt on a worldwide basis<sup>7</sup>. Thus, in addition to providing domestic energy alternatives, investment in hydrogen energy research will result in opportunities for U.S. technologies in over-seas markets.

### **Currently Available Hydrogen Storage Technologies**

Hydrogen can be made available on-board vehicles in containers of compressed or liquefied H<sub>2</sub>, in metal hydrides, or by gas-on-solid adsorption. Hydrogen can also be generated on-board by reaction or decomposition of a hydrogen containing molecular species<sup>8</sup>. Although each method possesses desirable characteristics, no approach satisfies all of the efficiency, size, weight, cost and safety requirements for transportation or utility use. The D.O.E. energy density goals for vehicular hydrogen storage call for systems with 6.5 wt % H<sub>2</sub> and 62 kg H<sub>2</sub>/m<sup>3</sup>.

Gas-on-solid adsorption is an inherently safe and potentially high energy density hydrogen storage method that should be more energy efficient than either chemical or metal hydrides, and

compressed gas storage. Consequently, the hydrogen storage properties of high surface area "activated" carbons have been extensively studied<sup>9,10,11</sup>. However, activated carbons are ineffective in hydrogen storage systems because only a small fraction of the pores in the typically wide pore-size distribution are small enough to interact strongly with gas phase hydrogen molecules.

The first measurements of hydrogen adsorption on carbon single-wall nanotubes (SWNTs) were performed here at NREL with highly impure samples. The room-temperature stabilization that was demonstrated at atmospheric pressures suggested the possibility of 5-10 wt % hydrogen storage in SWNT-based systems<sup>1</sup>. Contradictory results from purified SWNTs indicated that such high storage densities could only be achieved with cryogenic temperatures (80 K) and high pressures (158 atm)<sup>12</sup>, consistent with theoretical consideration of van der Waals interactions between H<sub>2</sub> and SWNTs<sup>13,14,15</sup>. However, we showed last year that SWNTs can adsorb between 3.5 and 4.5 wt% at room temperature and room pressure when un-optimized preparation procedures were employed<sup>16</sup>, and large-diameter SWNTs were recently shown to adsorb 4.2 wt % hydrogen at room temperature and ~100 atm<sup>17</sup>. This year we show that hydrogen storage densities can be optimized to values as high as 7 wt%, and present results from experiments designed to elucidate the mechanisms responsible for the unique hydrogen adsorption properties.

### **Technical Approach and Summary of Past Work**

We have been working on the idea that aligned and self-assembled single wall carbon nanotubes could serve as ideal hydrogen adsorbents since 1993. The concept was motivated by theoretical calculations<sup>18</sup> which suggested that adsorption forces for polarizable molecules within SWNTs would be stronger than for adsorption on ordinary graphite. Thus, high H<sub>2</sub> storage capacities could be achieved at relatively high temperatures and low pressures as compared to adsorption on activated carbons.

In the Proceedings of the 1994 Hydrogen Program Review, we presented microbalance data which demonstrated gravimetric hydrogen storage densities of up to 8.4 wt% at 82 K and 570 torr on samples containing carbon nanotubes. This substantial uptake at low hydrogen pressures demonstrated the strong interaction between hydrogen and these materials, consistent with higher heats of adsorption than can be found with activated carbons.

In the 1995 Hydrogen Program Review Proceedings, we presented the results of our temperature programmed desorption (TPD) studies which showed significant H<sub>2</sub> adsorption near room temperatures. The adsorption energies on nanotube materials were estimated to be a factor of 2-3 times higher than the maximum that has been observed for hydrogen adsorption on conventional activated carbons. These were the first results which demonstrated the existence of stable adsorbed hydrogen *on any type of carbon at temperatures in excess of 285 K*. We also analyzed the nanotube production yields versus rod translation rate in the electric arc.

In 1996 we performed a detailed comparative investigation of the hydrogen adsorption properties of SWNT materials, activated carbon, and exfoliated graphite. We also determined that the cobalt nanoparticles present in the arc-generated soots do not play a role in the observed hydrogen uptake. We determined the amount of hydrogen which is stable at near room

temperatures on a SWNT basis is between 5 and 10 wt%, and found that an initial heating in vacuum is essential for producing high temperature hydrogen adsorption. Further experiments suggested that SWNTs are selectively opened by oxidation during this heating, and that H<sub>2</sub>O is more selective in oxidation than O<sub>2</sub> due to hydrogen termination of dangling bonds at the edges of opened nanotubes. Purposeful oxidation in H<sub>2</sub>O resulted in hydrogen storage capacities which were improved by more than a factor of three. We also correlated the measured nanotube densities produced by specific synthesis rod translation rates during arc-discharge with hydrogen storage capacities determined by TPD. Finally, we utilized NREL's High Flux Solar Furnace to form nanotubes by a new and potentially less expensive route for the first time.

In 1997, the desorption of hydrogen was found to fit 1st order kinetics as expected for physisorbed H<sub>2</sub>, and the activation energy for desorption was measured to be 19.6 kJ/mol. This value is approximately five times higher than the value expected for desorption of H<sub>2</sub> from planar graphite and demonstrates that SWNT soots can provide very stable environments for H<sub>2</sub> binding. We also employed diffuse reflectance Fourier transform infrared (DRFTIR) spectroscopy to determine the concentrations and identities of chemisorbed species bound to the carbon surface as a function of temperature, and determined that "self-oxidation" allows high-temperature adsorption of hydrogen to occur in the arc-generated SWNT materials. We also began synthesizing SWNT materials in much higher yield than is currently possible with arc-discharge by using a laser vaporization process. We determined that the very long SWNTs made by this method could not be activated towards high-temperature H<sub>2</sub> physisorption by the same oxidative methods that were found to be effective for tubes produced by arc-discharge.

In 1998 we made significant advances in synthesis and characterization of SWNT materials so that we could prepare gram quantities of SWNT samples and measure and control the diameter distribution of the tubes by varying key parameters during synthesis. By comparing continuous wave (c.w.) and pulsed laser techniques, we learned that it is critical to stay in a vaporization regime in order to generate SWNTs at high yield. We also developed methods which somewhat purified the nanotubes and cut them into shorter segments. We performed temperature programmed desorption spectroscopy on high purity carbon nanotube material obtained from our collaborator Prof. Patrick Bernier, and finished construction of a high precision Sievert's apparatus which will allow the hydrogen pressure-temperature-composition phase diagrams to be evaluated for SWNT materials.

Last year we improved our laser-based method so that material containing between 20 - 30 wt% SWNTs could be generated at a rate of ~ 150 mg/hr or ~ 1.5 g/day. A simple 3-step purification technique was developed which resulted in single walled carbon nanotubes of greater than 98 wt% purity. A thermal gravimetric analysis (TGA) method was developed to allow the accurate determination of nanotube wt% contents in carbon soots. We also established a process for reproducibly cutting purified laser-generated materials. This advance was necessary since laser-produced tubes were found to be unresponsive to the oxidation methods that successfully opened arc-generated tubes. TPD spectroscopy demonstrated that purified cut SWNTs adsorbed between 3.5 – 4.5 wt% hydrogen under ambient conditions in several minutes and that the adsorbed hydrogen was effectively "capped" by CO<sub>2</sub>

This year we present the details of the new cutting procedure and show that, when optimized, hydrogen storage densities up to 7 wt% can be achieved. Infrared absorption spectroscopy measurements on pristine and H<sub>2</sub>-charged samples indicate that no C-H bonds are formed in the hydrogen adsorption process. These experiments are in agreement with an earlier temperature programmed desorption analysis which showed that hydrogen molecules are not dissociated when bound to the SWNT surfaces<sup>1</sup>. This conclusion is further supported by first neutron scattering measurements of hydrogen adsorbed onto SWNTs which were performed through collaboration with researchers at NIST and University of Pennsylvania<sup>2</sup>. We also developed methods to tune SWNT diameters during synthesis so that mechanistic aspects of H<sub>2</sub> storage can be probed<sup>3</sup>, and learned how to de-tangle and organize individual tubes to form "superbundles" that will afford high volumetric storage densities<sup>4</sup>. Finally, we wish to report that we have performed first synthesis experiments with a new laser which recently arrived at NREL. Raman spectroscopy indicated that the as-produced materials were ~ 50 wt% pure SWNTs, in contrast to the 20 to 30 wt% usually seen with the previous laser, and the production rate for raw soot appears to be significantly greater than the 150 mg/hr observed previously, even though the current performance is probably far from optimal.

## Experimental

### Pulsed Laser Synthesis of SWNTs

SWNT materials were synthesized by a laser vaporization method similar to that of Thess et al.<sup>19</sup>. A single Molelectron MY35 Nd:YAG laser was used which produced gated laser light ranging in duration from 300 to 500 ns at a frequency of 10 Hz. The gated laser light contained numerous short laser pulses of about 5 to 15 ns. The emission wavelength was 1064 nm at an average power of 20 - 30 W/cm<sup>2</sup>. An electronically rastered beam enabled material generation at rates of 75 - 150 mg / h. Typically, production is ~ 1.5 g / day. It is important to stay in a vaporization regime<sup>20</sup> during synthesis so that graphite particles are not ejected. Targets were made by pressing powdered graphite (~ 1 μ particle size) doped with 0.6 at % each of Co and Ni in a 1 1/8" inch dye at 10,000 psi. Crude soot was produced between 850 - 1200 °C with 500 Torr Ar flowing at 100 sccm. Raw materials were estimated to contain ~ 20 - 30 wt% SWNTs by both a detailed analysis of numerous different TEM images<sup>20</sup> and an accurate thermal gravimetric analysis method. SWNT diameters were between 1.1 - 1.4 nm [3]. Inductively coupled plasma spectroscopy (ICPS) was performed after complete air-oxidation of the carbon soots and thorough digestion of the residue in concentrated HNO<sub>3</sub>. The same metal content was found in both the laser-generated crude and the initial target to be ~6 wt%.

### Purification of Laser-generated SWNTs

Approximately 80 mg of the above laser-generated crude was refluxed in 60 ml of 3M HNO<sub>3</sub> for 16 h at 120 °C. The solids were collected on a 0.2 μm polypropylene filter in the form of a mat and rinsed with deionized water. After drying, an ~ 82 wt % yield was obtained. The weight lost is consistent with the digestion of the metal and an additional ~ 12 wt % of the carbon impurities. The carbon mat was then oxidized in stagnant air at 550 °C for 10 min., leaving behind pure SWNTs. The SWNTs were shown to be > 98 wt% pure with thermal gravimetric

analysis. Also, TGA revealed that no significant SWNTs were consumed in the purification process<sup>21</sup>.

### **Cutting of Laser-generated SWNTs**

Purified 1-3 mg samples were sonicated in 20 ml of 4M HNO<sub>3</sub> with a high-energy probe for 10 minutes to 24 hrs at powers ranging from 25 – 250 W/cm<sup>2</sup>. Figure 1 displays a typical transmission electron microscopy (TEM) image of purified SWNTs following ultrasonication in 4M HNO<sub>3</sub> for 16 hrs, and shows that the very long ropes found after purification<sup>21</sup> have been cut and re-assembled. The large-scale cutting observed here is consistent with the generation of cuts and defects that have been observed by others<sup>22, 23, 24</sup>. We find that cutting with a high-energy probe in HNO<sub>3</sub> is necessary to achieve high-capacity ambient H<sub>2</sub> adsorption, explaining why other studies have not seen the high room-temperature capacities observed here.<sup>12</sup> Other TEM images of cut samples revealed metal particles ranging in size from several nanometers to several microns. X-ray patterns of the particles in the cut samples were consistent with an alloy of nominal composition TiAl<sub>0.1</sub>V<sub>0.04</sub> as expected for disintegration of the ultrasonic probe.

### **Temperature Programmed Desorption**

Details of the ultra high vacuum (UHV) chamber employed for the TPD studies have been reported previously<sup>1,8</sup>. Briefly, carbon samples weighing ~1 mg were placed in a packet formed from 25 μm thick platinum foil and mounted at the bottom of a liquid nitrogen cooled cryostat. The packet could be resistively heated with a programmable power supply. Pinholes in the foil enable gas diffusion into and out of the packet. An ion gauge and capacitance manometer are employed to monitor pressure. Gas exposures are controlled with a variable conductance leak valve. Isolation gate valves separate the sample compartment during high-pressure gas exposures. A mass spectrometer measures species with an m/e up to 300 a.m.u. and insures that only hydrogen is involved in adsorption/desorption cycles. Signals were sufficiently large that the ion current could provide low-noise spectra without multiplication. The instrument was easily calibrated<sup>25</sup> by thermally decomposing known amounts of CaH<sub>2</sub>. The amount of evolved hydrogen was linear with the weight of decomposed CaH<sub>2</sub>, and the calibrations were performed with amounts of CaH<sub>2</sub> that yielded a TPD signal similar to the SWNT samples. The charged hydrogen could also be desorbed under flowing helium during thermal gravimetric analysis (TGA). The hydrogen uptake measured by TPD and TGA was within 10%. Samples were initially degassed by heating in a vacuum of ~ 10<sup>-7</sup> torr to 823 - 973 K at 1 K/s. The sample temperature was measured with a thin thermocouple spot-welded to the platinum packet. Room temperature H<sub>2</sub> exposures for ~ 1 minute at pressures between 10–500 torr saturated the hydrogen adsorption. Capacity determinations in the TPD were done by cooling the sample to 130 K prior to evacuation of the chamber.

### **Infrared Absorption Spectroscopy**

Transmission Fourier transform infrared (FTIR) studies of single walled carbon nanotubes were performed on a Nicolet 690 spectrometer with a liquid nitrogen cooled MCT-B detector at a resolution of 4 cm<sup>-1</sup>. Thin SWNT films were prepared employing an Anthem airbrush to spray SWNT/acetone mixtures onto silicon wafers. Approximately 4 mg of various SWNT materials

were suspended in ~ 15 ml acetone by sonication with an ultra sonic probe for several minutes. The resulting solution was sprayed onto the silicon for ~ 10 s. at 30 p.s.i., and the acetone was allowed to evaporate at room temperature in air. A uniform thin SWNT film on the IR transparent silicon substrate was thus obtained. Infrared spectra were ratioed to a background spectrum of a clean silicon wafer. A minimum of 500 scans were collected.

## Results and Discussion

### Hydrogen Adsorption on Cut SWNTs

Upon degassing the purified cut SWNT samples in vacuum, the high capacity hydrogen adsorption was activated. Figure 2 displays the H<sub>2</sub> TPD spectrum of a degassed sample following a brief room temperature H<sub>2</sub> exposure at 500 torr. The spectrum is characterized by two separate desorption signals peaked at ~ 375 and 600 K indicating at least two different types of sites for hydrogen adsorption. The peak desorption temperatures of these signals can be as much as 100 K lower depending on the SWNT sample and the specific cutting conditions. The hydrogen adsorption capacity, as measured by calibrated TPD, was ~ 6.5 wt% on a total sample weight basis after sonication for 16 hrs at 50 W/cm<sup>2</sup> and degassing to 825 K. This sample was found to contain ~ 15 wt% TiAl<sub>0.1</sub>V<sub>0.04</sub> by combusting the carbon fraction in flowing air and accounting for the oxidation of the metals. In addition to being used in the construction of ultrasonic probes, TiAl<sub>0.1</sub>V<sub>0.04</sub> is also employed in fusion reactor components. The latter application has led to numerous studies of the interactions between the alloy and hydrogen. A maximum of ~3 wt % hydrogen is observed<sup>26,27,28</sup>, while virtually no adsorption is seen for T < 373 K due to poor kinetics<sup>28</sup>. We generated TiAl<sub>0.1</sub>V<sub>0.04</sub> samples with the ultrasonic probe for 16 hrs in 4M HNO<sub>3</sub> without the addition of SWNTs. The generated particles exhibited X-ray patterns consistent with the alloy found in the SWNT samples. After a normal degas and H<sub>2</sub> exposure, the TiAl<sub>0.1</sub>V<sub>0.04</sub> sample exhibited only ~ 2.5 wt% hydrogen adsorption as measured by both TPD and volumetric techniques. Assuming that the alloy in the SWNT sample behaves like the pure alloy sample, the hydrogen uptake on the SWNT fraction is ~ 7.2 wt%. Samples with higher alloy contents had reduced overall hydrogen capacities, but the value of ~ 7 wt% on the SWNT fraction was relatively constant. The total adsorption capacity of the cut samples varied between 2-7 wt% depending on the material, the sonication power, sonication time, the hydrodynamics of the sonication vessel and the sample degas temperature. Adjustments in these parameters also affected the temperatures of the hydrogen desorption signals, but these results will be discussed in detail later<sup>29</sup>. The storage results were highly reproducible within 10-20% for a given set of experimental conditions. The samples are stable to cycling with no apparent degradation when the vacuum and the hydrogen are relatively clean and the sample temperature does not exceed ~825 K.

### Mechanism of Hydrogen Adsorption

We worked at length this past year to elucidate the mechanism of H<sub>2</sub> adsorption on SWNTs. This type of work is critical to the growing community that has been attempting to understand how SWNTs - as well as other types of nanostructured carbons - interact with hydrogen. There is considerable debate over the issue in the scientific community, and it is important to obtain a

deeper understanding so that; (i) accurate theoretical models and predictions may be developed, (ii) specific SWNT diameters and chiralities may be targeted for synthesis, and (iii) capacities and performance characteristics may be optimized. We have previously shown that hydrogen is not dissociated when adsorbed on arc-generated SWNTs even though the binding energy is 19.6 k/mol<sup>1</sup>. In this report we present new evidence that H<sub>2</sub> is non-dissociatively adsorbed on laser-generated materials. Additional evidence pointing at the true nature of the stabilizing interaction cannot be discussed here as this work has been submitted for publication elsewhere<sup>30</sup>. All-in-all, we find that the interaction between H<sub>2</sub> and single-wall nanotubes is mid-way between conventional van der Waals adsorption and chemical bond formation. A detailed understanding of the mechanism coupled with a high degree of control during synthesis should allow useful hydrogen adsorbents to be designed and constructed.

Figure 3 displays TPD data from a sample which displays hydrogen desorption peaks at ~ 425 and 600 K. The low-temperature peak occurs at a slightly higher temperature in comparison to the spectrum in Fig 2. due to the specifics of nanotube diameter and chirality and alterations in the cutting procedure. The hydrogen corresponding to the signal peaked at 425 K can be mostly evolved by holding the sample at room temperature overnight in vacuum, or completely evolved after 1 hr at 373 K (Fig. 3). Also in Fig. 3 it is apparent that all but the most stable hydrogen is liberated after heating in vacuum for 1 hr at 550 K. Qualitatively, the data show a distribution of binding energies for hydrogen, with the existence of at least two different sites.

Last year we learned that SWNT samples could be removed from vacuum after dosing with hydrogen and that the adsorbed hydrogen was retained on the sample<sup>31</sup>. Consequently, we are now able to perform spectroscopic experiments on H<sub>2</sub> charged samples outside of the controlled environment of the dosing chamber. Figure 4 displays infrared spectra of a cut and a cut, degassed and H<sub>2</sub> charged SWNT film. The spectrum of the cut sample displays a broad infrared absorbance between 942 and 1251 cm<sup>-1</sup> consistent with Si-O stretching vibrations due to slightly different concentrations in the native oxide layer of the silicon before and after coating with the cut SWNT film. Features at 1478 and 1630 cm<sup>-1</sup> which may be attributed to SWNT vibrational modes are also apparent. The feature at 1317 cm<sup>-1</sup> is consistent with an N-O stretching vibration attributed to the presence of intercalated HNO<sub>3</sub> species following cutting in nitric acid. Features between 2810 – 2970 cm<sup>-1</sup> consistent with C-H<sub>x</sub> stretching vibrations of chemisorbed hydrogen most likely introduced during cutting are also observed. Temperature programmed desorption data of the cut samples indicates that this chemisorbed hydrogen constitutes an amount less than 0.1 wt%. Following infrared spectroscopy the cut SWNT film was loaded into the TPD chamber, degassed to 550 °C and charged with hydrogen at 500 Torr. The amount of adsorbed hydrogen then corresponded to approximately 3.5 wt%. The infrared spectrum subsequently obtained for the charged SWNT sample displays a loss in the N-O stretching feature consistent with the desorption of intercalated nitric acid species during the degas (Fig. 4). However, a significant increase in the C-H<sub>x</sub> stretching region is not observed suggesting that the 3.5 wt% adsorbed hydrogen is not chemically bound to the nanotube walls. Changes in the infrared spectrum between 3100 - 3200 cm<sup>-1</sup> and at ~1600 cm<sup>-1</sup> are consistent with slightly different Si-OH and adsorbed H<sub>2</sub>O species present at different locations on the silicon substrate.

During the past year we also worked with collaborators at the National Institute of Standards and Technology and the University of Pennsylvania to perform inelastic neutron scattering



measurements on our hydrogen-loaded SWNT samples<sup>2</sup>. Figure 5 shows the signal associated with the ortho to para conversion as a function of temperature for the unprocessed material. Surprisingly the transition is observed at temperatures as high as 65K, indicating a binding energy of  $\sim 6$  kJ/mol. These first measurements were performed on raw (unpurified and uncut) SWNT samples grown by laser vaporization, and the dosing and degassing procedures were not fully controlled. Although we do not expect to see strongly-bound H<sub>2</sub>, these experiments serve as a basis for future work on samples which have been more carefully activated and charged with hydrogen. The reader is referred to the publication<sup>2</sup> for a detailed explanation of these neutron scattering measurements.

### **Diameter Tuning and Increased Production Rates by Controlled Laser Vaporization**

This year we have demonstrated, for the first time, that SWNT diameter distributions can be tuned through variation in laser pulse power. This advance is important to furthering progress towards the goals of the Hydrogen Program since there is growing evidence in our lab as well as in others<sup>17</sup> that the diameter of a given SWNT can effect the capacity, thermodynamics, and kinetics of hydrogen storage. The production of SWNTs was investigated at room temperature with a porous target, and at 1200 °C with a dense target. The tube diameters were shifted to smaller sizes with increasing pulse power in both cases. The SWNT size distributions and yields were studied with Raman spectroscopy and transmission electron microscopy, and the evolution of the material quality with laser energy parameters was investigated. The smaller fragments generated by the higher peak pulse powers result in the formation of smaller tubes. Conversely, larger tubes are generated when larger fragments are produced at lower peak pulse powers. The overall yield of nanotubes is low unless thermal energy for assembly is provided by an external furnace. The study offers a unique view of SWNT formation mechanisms, and should aid in the development methods for the rational control of SWNTs. The full, peer-reviewed study was recently published in Chemical Physics Letters<sup>3</sup>. Some key findings are reproduced here.

A Molelectron Nd:YAG laser was operated in both a Q-switched (10 ns) and long-pulsed (450 ns) mode. The pulse repetition rate was fixed at 10 Hz, and experiments were performed with an external furnace surrounding the target at a temperature of 1200 °C. Figure 6 shows Raman spectra in the radial breathing mode region for SWNT materials produced with three different types of laser pulses. Spectrum 6a shows data from material produced at an average power of 200 W/cm<sup>2</sup> in long-pulse mode where the pulse power is 45 MW/cm<sup>2</sup>. Three signals are present at 164, 177 and 182 cm<sup>-1</sup> consistent with populations of (10,10), (16,0), and (9,9) tubes<sup>32</sup>. Much weaker signals at 193 and 202 cm<sup>-1</sup> may also be discerned. The Raman spectrum is dramatically shifted to higher frequencies corresponding to smaller tubes when the average power is maintained at 200 W/cm<sup>2</sup> but the laser is Q-switched to yield a pulse power of 2 GW/cm<sup>2</sup> (Fig 6b). The 164 cm<sup>-1</sup> peak is no longer observed, and the signals at 177 and 182 cm<sup>-1</sup> are significantly reduced in intensity. Two new strong bands found at 202 and 193 cm<sup>-1</sup> can be associated with (8,8) tubes and a slightly larger non-armchair tube such as the (14,0) tube, respectively.

The data is consistent with the shift to smaller tubes seen with increasing peak pulse power in room temperature experiments<sup>3</sup>. However, with the Molelectron laser, the comparison can be made at different peak powers when the average power and pulse repetition rate are the same.

The shift to smaller tubes is clearly due to the increased pulse power. The point is proven further by considering the size distribution of SWNTs when the average power, and thus the pulse power, are reduced while the pulse width and repetition rate are held constant. Figure 6c shows the radial breathing modes for SWNTs produced at an average power of 80 W/cm<sup>2</sup> and a 10 ns pulse width so the peak power is 0.8 GW/cm<sup>2</sup>. The SWNT size distribution is shifted to larger values in comparison to the distribution obtained at a peak power of 2 GW/cm<sup>2</sup>, and is in fact similar to the size distribution found at an average power of 200 W/cm<sup>2</sup> in the long-pulse mode. Two major features are present at 164 and 182 cm<sup>-1</sup> as expected for (10,10) and (9,9) tubes, and weaker modes at 193 and 202 cm<sup>-1</sup> are also seen.

In addition to learning how to control nanotubes size distributions we have also learned how to de-tangle and order nanotubes on a larger scale. This capability eventually may be important for achieving high packing densities, and therefore high volumetric hydrogen storage densities. Figure 7 shows a SWNT "superbundle" prepared using our methods. The relevant discussion is beyond the scope of this report, but is reported completely in an article published in Chemistry of Materials<sup>4</sup>.

Finally, we wish to report that we have performed the first synthesis experiments with a new laser which recently arrived at NREL. The Molelectron MY35 laser which had been in use was more than 20 years old and had been failing more and more regularly. Additionally problematic was the fact that the laser spot itself was very inhomogenous and irreproducible after required flash lamp changes. The TEM images of Figure 8 show the quality of the raw materials produced using a) old Molelectron MY35 and b) the new Light Age, Inc., laser operating at ~ 0.5 J/pulse. Raman spectroscopy indicated that the as-produced materials were ~ 50 wt% pure SWNTs, in contrast to the 20 to 30 wt% usually seen with the Molelectron laser. The new laser will be much more stable and require less maintenance than the Molelectron laser, and the production rate for raw soot appears to be significantly greater than the 150 mg/hr observed previously, even though the current performance is probably far from optimal. The fact that we can easily produce gram quantities of this quality material everyday will greatly facilitate our development of a carbon nanotube based hydrogen storage system.

### **Conclusions / Future Work**

This year we have presented the details of our recently developed cutting procedure for laser generated SWNTs and have shown that, when optimized, hydrogen storage densities up to 7 wt% can be achieved. Briefly, purified 1 - 3 mg samples are sonicated in 20 ml of 4M HNO<sub>3</sub> with a high-energy probe for 16 hrs at a power of 50 W/cm<sup>2</sup>. We have employed TPD measurements to show that at least two unique binding sites are present for hydrogen adsorption on SWNTs. We have also employed infrared absorption spectroscopy measurements on pristine and H<sub>2</sub>-charged samples to show that no C-H bonds are formed in the hydrogen adsorption process. These experiments are in agreement with an earlier temperature programmed desorption analysis which showed that hydrogen molecules are not dissociated when bound to the SWNT surfaces<sup>1</sup>. This conclusion is further supported by the first neutron scattering measurements which were performed through collaboration with researchers at NIST and University of Pennsylvania<sup>2</sup>. We also developed methods to tune SWNT diameters during

synthesis so that mechanistic aspects of H<sub>2</sub> storage can be probed<sup>3</sup>, and learned how to de-tangle and organize individual tubes to form "superbundles" that will afford high volumetric storage densities<sup>4</sup>. Finally, we wish to report that we have performed the first synthesis experiments with a new laser which recently arrived at NREL. The as-produced materials are ~ 50 wt% pure SWNTs, in contrast to the 20 to 30 wt% usually seen with the old laser, and the production rate for raw soot appears to be significantly greater than the 150 mg/hr observed previously, even though the current performance is probably far from optimal.

The fact that we can easily produce gram quantities of ~ 50 wt% SWNT material everyday will facilitate future large-scale measurements with volumetric techniques. These experiments will more closely simulate the anticipated on-board hydrogen storage system. In the future we will also employ our laser diameter tuning techniques to better establish a correlation between materials properties and hydrogen adsorption behaviors. For example, is the adsorption site that may be depopulated at 300 K for cut and purified laser-generated SWNTs located on larger diameter tubes rather than smaller diameter tubes? Is it also possible that either semi-conducting or metallic SWNTs are better suited for hydrogen adsorption? Raman studies at multiple wavelengths which enable the differentiation between semi-conducting and metallic nanotubes<sup>33</sup> may enable an answer to this question. If a preference is determined, synthetic methods for the production of specifically metallic or semiconducting tubes will need to be developed. Our current state of the art production and purification techniques provide gram quantities of high quality material per day. We will of course continue to focus on up-scaling the production and purification of SWNT adsorbent materials.

## References

- (1) Dillon, A.C., Jones, K.M., Bekkedahl, T.A., Kiang, C.H., Bethune, D.S. and Heben, M.J., *Nature* **1997**, 386, 377.
- (2) Brown, C.M., Yildirim, T., Neumann, D.A., Heben, M.J., Gennett, T., Dillon, A.C., Alleman, J.L. and Fischer, J.E., *Chem. Phys. Lett.* **2000**, 329, 311.
- (3) Dillon, A.C., Parilla, P.A., Alleman, J.L., Perkins, J.D. and Heben, M.J., *Chem. Phys. Lett.* **2000**, 316, 13.
- (4) Gennett, T., Dillon, A.C., Alleman, J.L., Hassoon, F.S., Jones, K.M. and Heben, M.J., *Chem. of Mat.* **2000**, 12, 599.
- (5) Cannon, J.S. in *Harnessing Hydrogen* INFORM, Inc., New York, **1995**
- (6) N.E.S., **1991/1992**,
- (7) Flavin, C. and Lessen, N. in *Power Surge* W.W. Norton & Co., New York, **1994**
- (8) Dillon, A.C., Bekkedahl, T.A., Cahill, A.F., Jones, K.M. and Heben, M.J. *Carbon Nanotube Materials for Hydrogen Storage* 1-521 (Coral Gables, FL, 1995).
- (9) Carpetis, C. and Peschka, W., *Int. J. Hydrogen Energy* **1980**, 5, 539.
- (10) Schwarz, J.A. *Modification Assisted Cold Storage (MACS)* .
- (11) Schwarz, J.A. *Activated Carbon Based Storage System* 1-271 (Honolulu, HI., 1992).
- (12) Ye, Y., Ahn, C.C., Witham, C., Fultz, B., Liu, J., Rinzler, A.G., colbert, D., Smith, K.A. and Smalley, R.E., *Appl. Phys. Lett.* **1999**, 74, 2307.
- (13) Wang, Q. and Johnson, J.K., *J. Phys. Chem.* **1999**, 103, 4809.

- (14) Wang, Q. and Johnson, J.K., *J. Chem Phys.* **1999**, *110*, 577.
- (15) Rzepka, M., Lamp, P. and de la Casa-Lillo, M.A., *J.Phys. Chem* **1998**, *102*, 10894.
- (16) Dillon, A.C., Gennett, T., Alleman, J.L., Jones, K.M., Parilla, P.A. and Heben, M.J. *Carbon Nanotube Materials for Hydrogen Storage* (San Ramon, CA, 2000).
- (17) Liu, C., Fan, Y.Y., Liu, M., Cong, H.T., Cheng, H.M. and Dresselhaus, M.S., *Science* **1999**, *286*, 1127.
- (18) Pederson, M.R. and Broughton, J.Q., *Phys. Rev. Lett.* **1992**, *69*, 2689.
- (19) Thess, A., Lee, R., Nikolaev, P., Dai, H., Pitit, P., Robert, J., Xu, C., Lee, Y.H., Kim, S.G., Rinzler, A.G., Colbert, D.T., Scuseria, G.E., Tomanek, D., Fischer, J.E. and Smalley, R.E., *Science* **1996**, *273*, 483.
- (20) Dillon, A.C., Parilla, P.A., Jones, K.M., Riker, G. and Heben, M.J., *Mater. Res. Soc. Conf. Proc.* **1998**, *526*, 403.
- (21) Dillon, A.C., Gennett, T., Jones, K.M., Alleman, J.L., Parilla, P.A. and Heben, M.J., *Adv. Mat.* **1999**, *11*, 1354.
- (22) Shelimov, K.B., Esenaliev, R.O., Rinzler, A.G., Huffman, C.B. and Smalley, R.E., *Chem. Phys. Lett.* **1998**, *282*, 429.
- (23) Liu, J., Rinzler, A.G., Dai, H., Hafner, J.H., Bradley, K.R., Boul, P.J., Lu, A., Iverson, T., Shelimov, K., Huffman, C.B., Roderiguez-Macias, F., Shon, Y.-S., Lee, T.R., Colbert, D.T. and Smalley, R.E., *Science* **1998**, *280*, 1253.
- (24) Lu, K.L., Lago, R.M., Chen, Y.K., Green, M.L.H., Harris, P.J.F. and Tsang, S.C., *Carbon* **1996**, *34*, 814.
- (25) Wang, J. and McEnaney, B., *Thermochimica Acta.* **1991**, *190*, 143.
- (26) Davis, J.W. and Smith, D.L., *J. Nuc. Mat.* **1979**, *85*, 71.
- (27) Jiao, J. and Seraphin, S., *J. Mater. Res.* **1998**, *13*, 2438.
- (28) S. Ishiyama, K. Fukaya, M. Eto and Miya, N., *Journal of Nuclear Science and Technology* **2000**, *37*, 144.
- (29) Gennett, T., Dillon, A.C., Alleman, J.L., Parilla, P.A., Jones, K.M. and Heben, M.J., ( *in preparation* )
- (30) Dillon, A.C., Gennett, T., Alleman, J.A., Jones, K.M., Parilla, P.A. and Heben, M.J., ( *submitted to Nature* )
- (31) Dillon, A.C., Gennett, T., Alleman, J.L., Jones, K.M., Parilla, P.A. and Heben, M.J. *Carbon Nanotube Materials for Hydrogen Storage* (Herndon, VA, 1999).
- (32) Rao, A.M., Richter, E., Bandow, S., Chase, B., Eklund, P.C., Williams, K.A., Fang, S., Subbaswamy, K.R., Menon, M., Thess, A., Smalley, R.E., Dresselhaus, G. and Dresselhaus, M.S., *Science* **1997**, *275*, 187.
- (33) Brown, S.D.M., Corio, P., Marucci, A., Dresselhaus, M.S., Pimenta, M.A. and Kneipp, K., *Phys. Rev. B* **2000**, *61*, R5137.

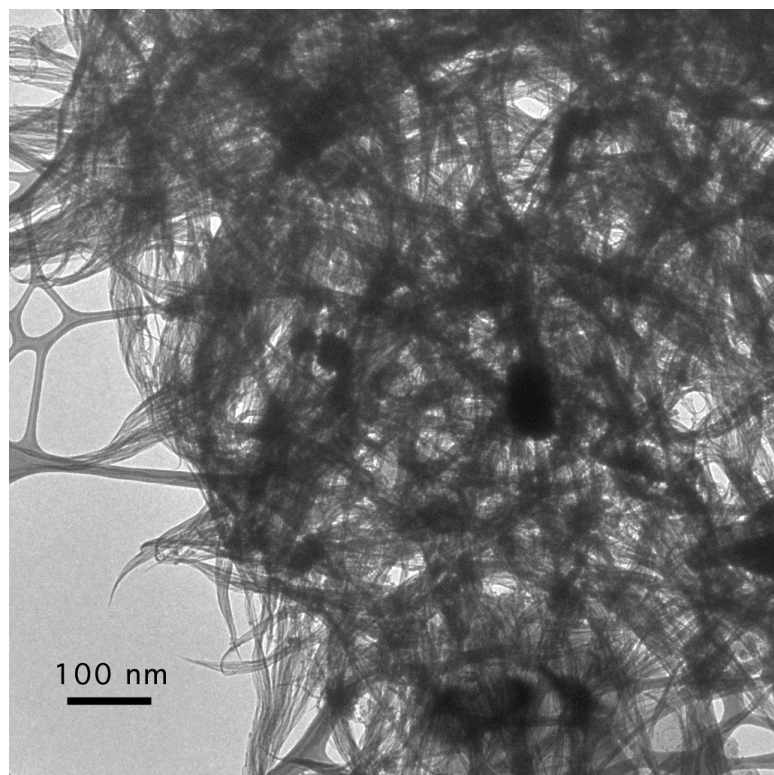


**Figure 1:** TEM image of purified SWNTs following ultrasonication in 4M HNO<sub>3</sub> for 16 hrs.

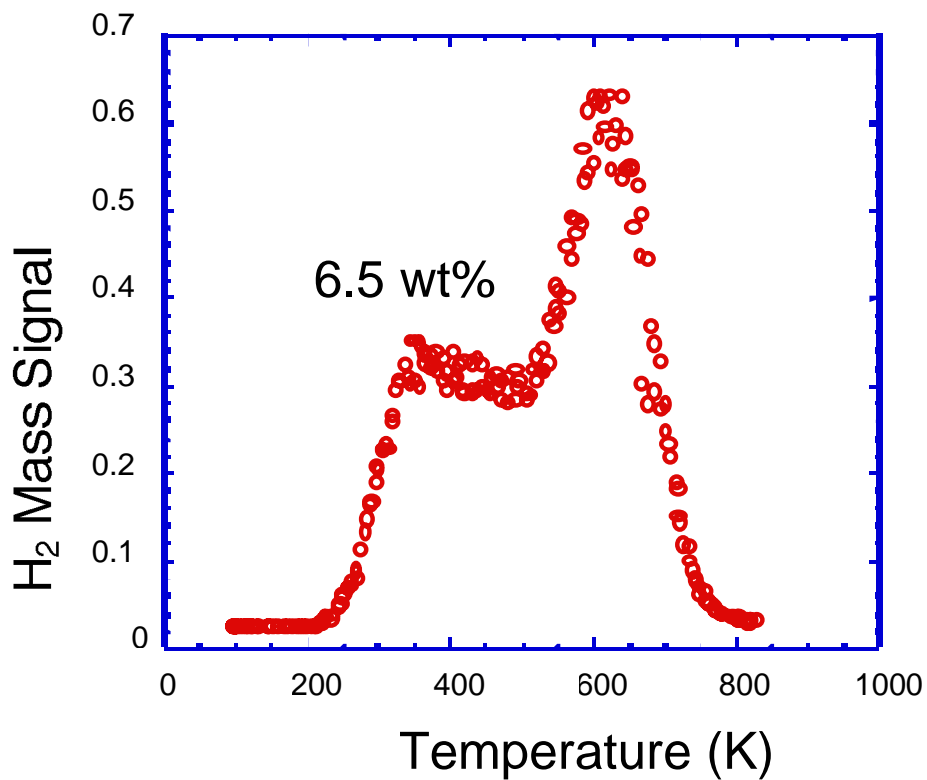


**Figure 2:** Hydrogen TPD spectrum of a degassed sample following a brief room temperature H<sub>2</sub> exposure at 500 torr. The adsorbed hydrogen corresponds to 6.5 wt%.

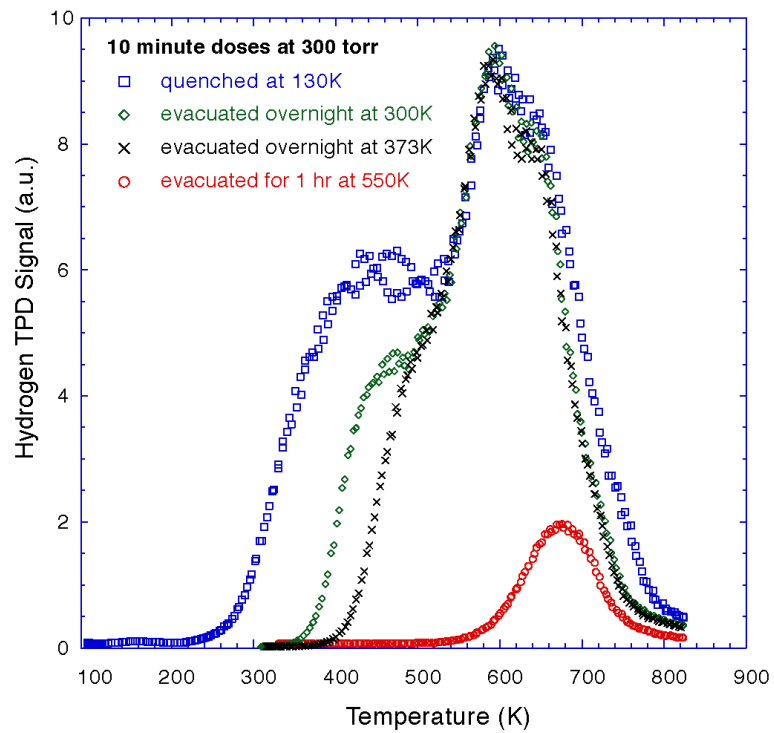


**Figure 3:** Hydrogen TPD data from an SWNT sample that was exposed to hydrogen at 300 Torr for 10 minutes followed by a variation in post-dosing conditions.

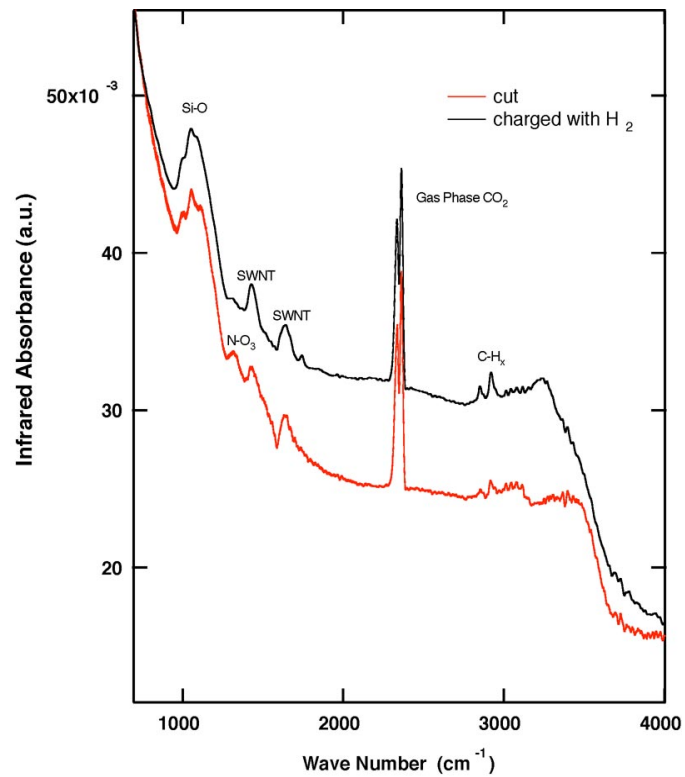


**Figure 4:** FTIR spectra of a cut and a cut, degassed and H<sub>2</sub> charged SWNT film.



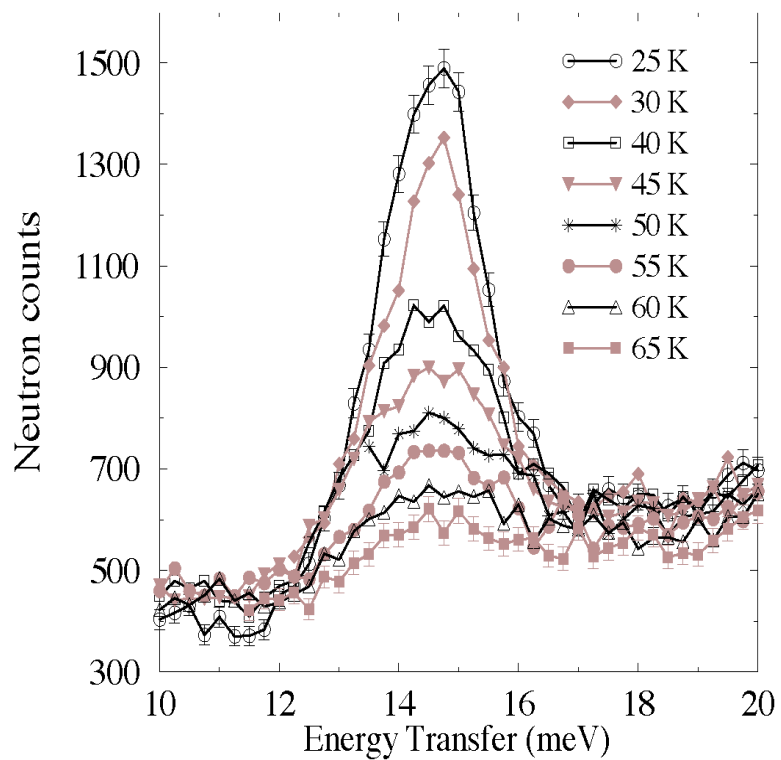


**Figure 5:** The signal from inelastic neutron scattering measurements on our hydrogen-loaded SWNT samples associated with the ortho to para conversion as a function of temperature.

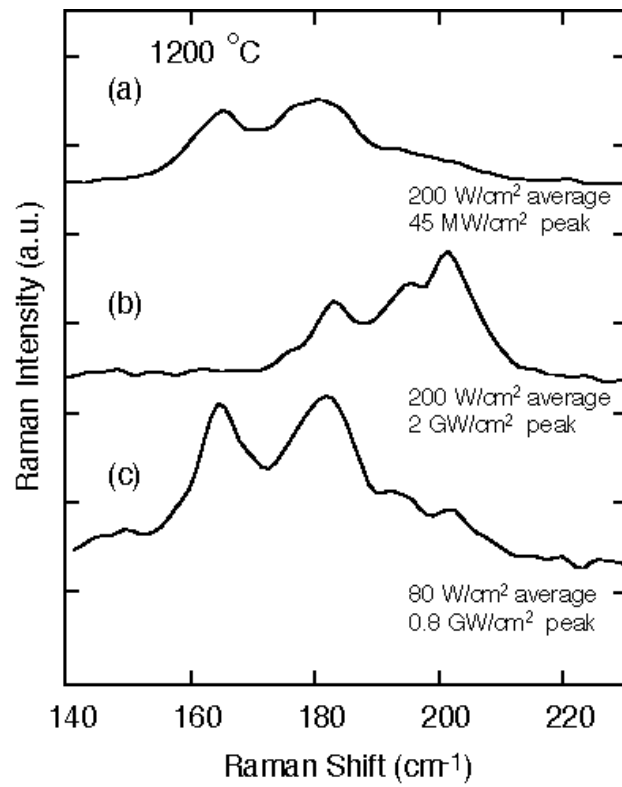


**Figure 6:** Raman spectra in the radial breathing mode region for SWNT materials produced with three different types of laser pulses.

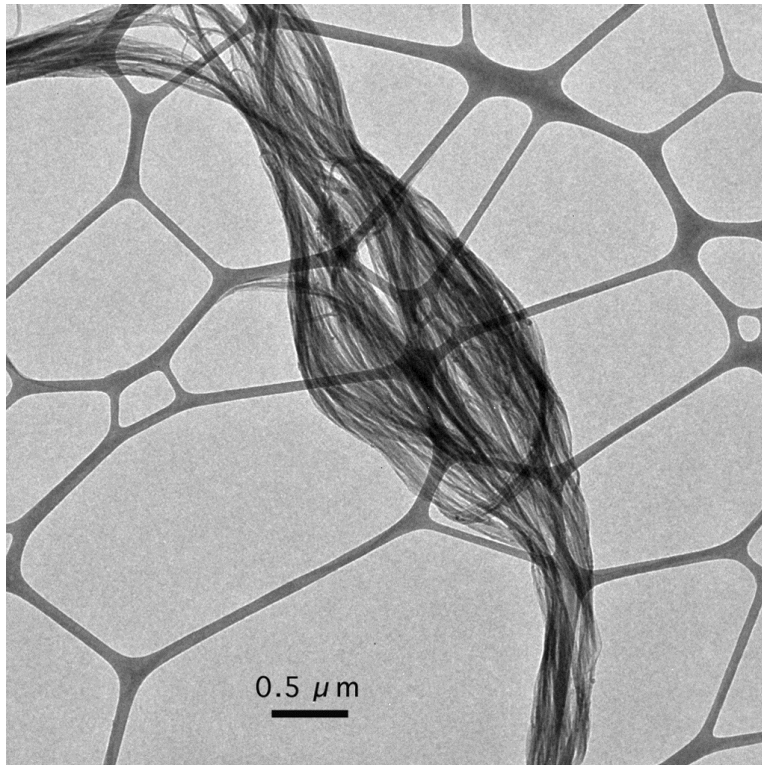


**Figure 7 :** An SWNT "superbundle". The large bundle of well-aligned tubes should enable higher capacity hydrogen storage.

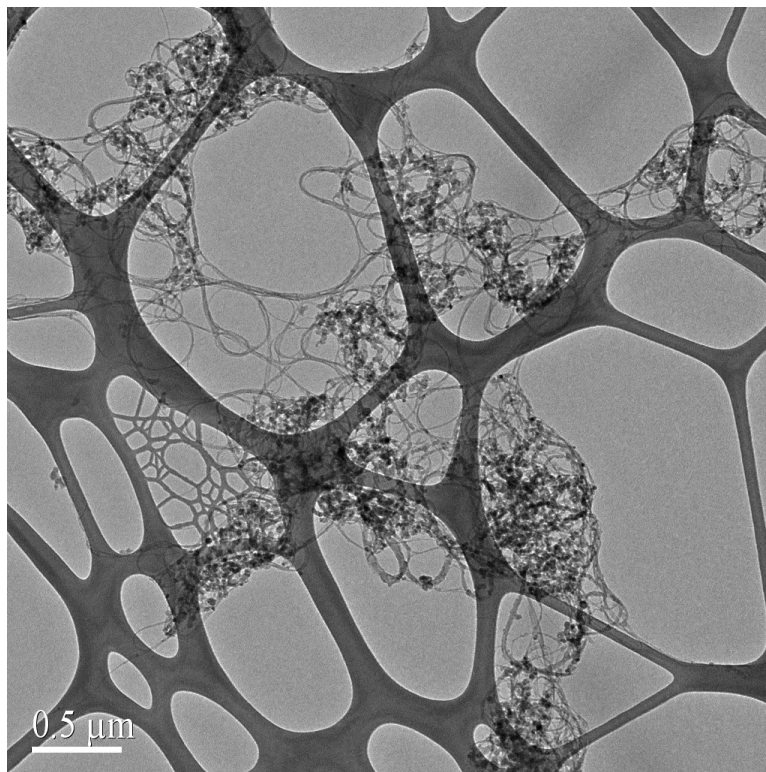
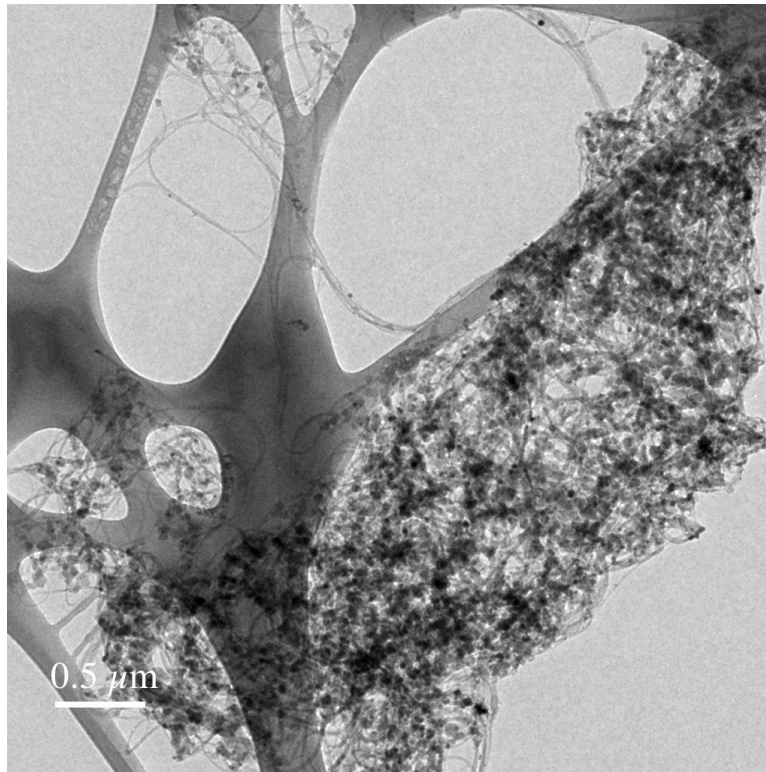


**Figure 8:** TEM images of the raw materials produced using a) the old Molelectron MY35 laser and b) the new Light Age, Inc. laser. The SWNT density was improved from ~20-30 wt% to 50 wt%.